Oxymyohemerythrin: discriminating between O2 release and autoxidation

By: Christopher R. Lloyd, Gregory M. Raner, Alicia Moser, Edward M. Eyring, and Walther R. Ellis Jr.

Lloyd, C.R., G.M. Raner, A. Moser, E.M. Eyring, and W.R. Ellis, Jr.Oxymyohemerythrin:Discriminating Between O2 Release and Autoxidation.J. Inorg. Biochem. 81:293-300 (2000). DOI: 10.1016/S0162-0134(00)00093-3

Abstract

Myohemerythrin (Mhr) is a non-heme iron O_2 carrier (with two irons in the active site) that is typically found in the retractor muscle of marine 'peanut' worms. OxyMhr may either release O_2, or undergo an autoxidation reaction in which hydrogen peroxide is released and diferric metMhr is produced. The autoxidation reaction can also be promoted by the addition of certain anions to Mhr solutions. This work, using recombinant Themiste zostericola Mhrs, contrasts the results of environmental effects on these reactions. For the O_2 release reaction, $\Delta V^{\ddagger}$(21.5°C)=+28±3 cm^3 mol^{-1}, $\Delta H^{\ddagger}$(1 atm)=+22±1 kcal mol^{-1}, and $\Delta S^{\ddagger}$(1 atm)=+ 28±4 eu. The autoxidation reaction (pH 8.0, 21.5°C, 1 atm) displays different kinetic parameters: $\Delta V^{\ddagger}$=-8±2 cm3 mol-1, $\Delta H^{\ddagger}$=+24.1±0.7 kcal mol^{-1}, and $\Delta S^{\ddagger}$=+1±1 eu. Autoxidation in the presence of sodium azide is orders of magnitude faster than solvolytic autoxidation. The $\Delta V^{\ddagger}$ parameters for azide anation and azide-assisted autoxidation reaction are +15±2 and +59±2 cm^3 mol^{-1}, respectively, indicating that the rate-limiting steps for the Mhr autoxidation and anation reactions (including O_2 uptake) are not associated with ligand binding to the Fe2 center. The L103V and L103N oxyMhr mutants autoxidize ≈10^3–10^5 times faster than the wild-type protein, emphasizing the importance of leucine-103, which may function as a protein 'gate' in stabilizing bound dioxygen.

Keywords:

Myohemerythrin; Autoxidation; Non-heme iron; Kinetics

Article:

1. Introduction

Three general classes of O_2 carriers [1] have been intensively studied since their discoveries in the nineteenth century: hemoglobins, hemocyanins, and hemerythrins. The hemoglobins, the most widespread family of dioxygen carriers, utilize iron porphyrin cofactors in O_2 transport. Hemocyanins are binuclear copper proteins found in members of the mollusk and arthropod phyla. Hemerythrins contain binuclear non-heme iron active sites, and occur in members of four families of marine invertebrates. The coordination of molecular oxygen to the ferrous or cuprous deoxy centers in these proteins involves charge transfer from the metal(s), resulting in oxy adducts that are best described as containing either coordinated superoxide (hemoglobins) or coordinated peroxide (hemocyanins and hemerythrins).

The hemerythrin class of O_2 carriers consists of hemerythrin (Hr), an oligomer most commonly found in the coelomocytes of sipunculids (marine 'peanut' worms), and a monomeric analogue found in the retractor muscle of these worms, myohemerythrin (Mhr). A wealth of structural and reactivity information [2,3] makes these proteins, which contain an Fe–O–Fe active site per monomer, the best understood members of a growing family [4–10] of diiron-oxo proteins. X-ray structures [11–14] of Hrs and Mhrs indicate that the active site is embedded in the interior of a four-α-helix bundle, each of whose helices contributes ligands (five terminal His, one bridging Asp, one bridging Glu) to the diiron-oxo core. Referring to Fig. 1, Fe1 retains its six ligands in all

forms of Mhr, while Fe2 contains a coordination site that can be occupied by a variety of mono-, di-, and linear triatomic ligands, including dioxygen and azide.

Leucine-103 is conserved in the known amino acid sequences of Hrs and Mhrs. The side-chain methyl groups of this residue (see Fig. 1) are in van der Waal's contact with bound dioxygen in the Themiste dyscrita oxyHr X-ray structure [11], and also with bound azide in the Themiste

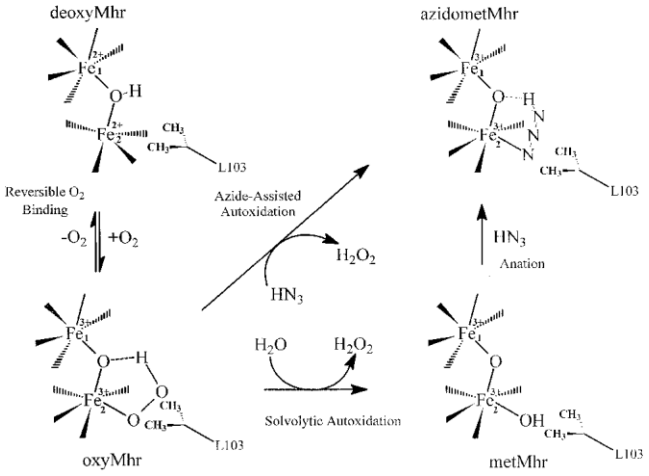

Fig. 1. Parallel pathways for the decay of oxymyohemerythrin: O_2 release (to produce deoxy-myohemerythrin vs. H_2O_2 release (autoxidation). The reactions that produce azidometmyohemerythrin, azide-assisted autoxidation and azide anation, are also indicated. The isopropyl side chain of leucine-103, that provides an important van der Waal's contact in oxyhemerythrin, is also shown.

zostericola azidometMhr [12] and T. dyscrita azidometHr [13] structures. Resonance Raman studies [15,16] and the polarized crystal spectrum [17] of oxyHr indicate that the bound peroxide is protonated (i.e. hydroperoxide), and that the ligand is hydrogen-bonded to the oxo bridge, as confirmed by the oxyHr X-ray structure. Sanders-Loehr and coworkers [15,18] have proposed that the proton involved in this hydrogen bond is derived from a bridging hydroxyl group in deoxyHr.

The refined X-ray crystal structures (1.6–2.0 Å) of various forms [11–14] of T. dyscrita Hr and T. zostericola Mhr are all apparently devoid of static channels for exogenous ligands to directly access Fe2 from the solvent. These crystallographic data prompted us to reinvestigate the uptake and release of O_2 by T. zostericola Mhr. We reported [19] our findings for these reactions, which do not exhibit the behavior expected for a single deoxyMhr+ O_2 ↔ oxyMhr equilibrium step, and we further suggested that the rate-determining steps for the uptake and release of O_2 do not coincide. As Fig. 1 indicates, oxyMhr (and oxyHr) can release O_2 (Eq. (1)) or undergo a normally much slower autoxidation reaction (Eq. (2)) that produces the met analogue:

$$\text{oxyMhr[Fe(III),Fe(III)]} \leftrightarrow \text{deoxyMhr[Fe(II),Fe(II)]} + O_2 \quad (1)$$

$$\text{oxyMhr[Fe(III),Fe(III)]} \leftrightarrow \text{metMhr[Fe(III),Fe(III)]} + H_2O_2 \quad (2)$$

The met analogue of the protein is incapable of binding O_2. The physiological importance of autoxidation is underscored by the isolation [20,21] of a cytochrome b_5–cytochrome b_5 reductase system in Phascolopsis gouldii that reduces metHr to the deoxy form.

The diiron-oxo unit of Mhr has elicited a considerable amount of attention from coordination chemists. The first accurate structural models [22,23] for metMhr appeared in 1983. The development of oxyMhr model complexes

[24– 27] has been more problematic, however.[3] Understanding the relationships between O_2 uptake and release on the one hand, and O_2 release and autoxidation on the other, is an important consideration in the rational design of a functional Mhr model complex.

In this report, we present kinetic results for reactions of the oxy and met forms of recombinant T. zostericola Mhrs. While release of O_2 is a kinetically straightforward process involving a rate-limiting Fe–O bond cleavage, autoxidation is more complex, displaying kinetic parameters which suggest the rate-determining step is not simply associative or dissociative. The rapid autoxidation of L103V and L103N oxyMhrs suggests that the Leu-103 side chain likely plays an important kinetic role by functioning not only as a 'gate' in oxygen uptake [19,28], but by stabilizing the oxy adduct relative to autoxidation through an important van der Waal's contact.

2. EXPERIMENTAL SECTION

2.1. Myohemerythrins

Recombinant T. zostericola wild-type metMhr was chromatographically purified [28] to homogeneity from Escherichia coli (BL-21 DE3) cell extracts. The L103V and L103N mutants were isolated as the apoproteins, stripped of adventitious metal ions, and reconstituted [28] with ferrous ammonium sulfate to produce the met forms. Contaminating apoproteins were removed by passage through a Whatman DE-52 ion-exchange column (sodium borate buffer, pH 9.0, μ =10 mM). For the wild-type and mutant proteins, purities were verified (>97%) by analytical isoelectric focusing, and Fe analyses (stoichiometries of 2±0.1 Fe per protein molecule were observed) were performed using a Perkin-Elmer 305A atomic absorption spectrometer.

DeoxyMhr samples were prepared from their met analogues by degassing on a vacuum manifold, followed by overnight reduction under argon with an excess of buffered sodium dithionite, which was subsequently removed by gel filtration chromatography. Wild-type oxyMhr was prepared just prior to use by exposure of deoxyMhr to the laboratory atmosphere; the purity of the oxyMhr was verified spectrophotometrically. The T. zostericola Mhrs are insoluble at their isoelectric points (pI values —7.6), requiring all studies to be carried out above this pH (Attempts to reconstitute wild-type apoMhr with iron salts below the pI were unsuccessful). Mhr samples for kinetic experiments were prepared in 300 mM Tris-sulfate buffers (pH 8.0) (Tris-chloride buffer interferes with kinetic measurements, particularly autoxidation reactions). The ionization constants of Tris exhibit negligible dependencies on pressure [29], and their known temperature dependencies [30] were taken into account in preparing buffers for the kinetic runs.

2.2. Kinetic measurements

The pH and temperature dependencies of the autoxidation kinetics of wild-type Mhr (samples were -70 μM) were obtained at atmospheric pressure using a Hewlett-Packard Model 8452A diode array spectrophotometer. The reaction was followed by monitoring the loss of the hydroperoxo→Fe^{III} ligand-to-metal charge-transfer transition, centered at 500 nm. The pressure dependence of the autoxidation kinetics was obtained using a quartz 'pill box' optical cell [31] (≈15 mm path length) contained within a pressurizable shroud [32], constructed of stainless steel and containing three sapphire windows. The shroud was seated into a Cary 2215 spectrophotometer that was equipped with an external thermostatting coil (±0.1°C) and was pressurized with liquid n-heptane between 1 and 1000 bar. No indications of pressure-induced protein denaturation or active site perturbations were observed in the optical spectra of the samples in this pressure range [19] (or even when pressurized to 2000 bar). Autoxidation data for wild-type oxyMhr were acquired for only two half-lives ($t_{1/2}$~19 h at 21.5°C) due to the slowness of these reactions. The autoxidations of the L103V and L103N oxyMhr mutants were followed (12°C, 1 bar, pH 8.0), owing to their rapidity, by reacting the deoxy proteins (0.2 mM) with O_2 (>0.4 mM) using the stopped-flow spectrophotometer described below, and observing the decays of the oxy intermediates to their respective met forms at 500 nm.

[3] A stable hydroperoxide adduct of a dinuclear Fe(III) complex at —78°C has been recently reported [27].

O_2 release reactions of wild-type oxyMhr, resulting in deoxyMhr formation, were studied (4–5 half-lives) using a custom-built stopped-flow spectrophotometer [19,33] that has a 10-ms dead time, and incorporates a syringe drive assembly and observation cell (500 nm monitoring wavelength) within a high-pressure vessel. The vessel was also fitted with an external thermostatting coil (±0.1°C) and pressurized with liquid n-heptane between 1 and 1000 bar. Sodium dithionite (25 mM; syringe 1) was used to scavenge O_2 from Mhr solutions (150 μM protein; 0.1 mM O_2; syringe 2), initiating O_2 release. Solutions in the syringes were allowed to equilibrate for at least 20 min after each pressure change. The temperature dependence of the O_2 release reaction (at 1 bar) was obtained using a Durrum stopped-flow spectrophotometer in which the reactant solutions were allowed to equilibrate for 1 h after each temperature change. The results of at least five reactions were averaged per data point reported herein.

Azidomet formation (wild-type Mhr) was followed (21.5°C, 1 bar, pH 8.0) using a Cary 2215 spectrophotometer (500 nm), for at least four half-lives, with azide in sufficient excess (>20 mM) over metMhr (30 μM) to ensure pseudo-first-order kinetics. The high pressure stopped-flow system, described above, was used to determine kinetic activation parameters for the azide anation and azide-assisted autoxidation reactions. In the latter case, azidometMhr formation was also monitored at 500 nm. (AzidometMhr has a strong azide→Fe^{III} ligand-to-metal charge-transfer transition band; the difference in the e500 for oxyMhr and azidometMhr is well characterized) [28]. Varying concentrations of azide were reacted with 90 μM protein (60 μM oxyMhr +30 μM metMhr) to produce the azidometMhr product.[4]

All kinetic data reported in this work were analyzed with KINFIT 3.0 software obtained from On-Line Instruments (Bogart, GA). Experimental uncertainties (estimated as ±one standard deviation from the mean) associated with individual points in Figs. 2–6 that do not contain error bars are contained within those points.

3. RESULTS

The reactions (pH 8.0, 12.0°C, 1 atm) of the deoxy L103V and L103N Mhrs with O_2 were both found to be biphasic. Stopped-flow traces (500 nm) of these reactions all display a rapid absorbance increase, due to formation of the respective oxyMhr intermediate, followed by a slower phase (attributed to autoxidation) that ultimately leads to a buildup of the met protein. More importantly, the decrease in OD500, due to formation of the L103V metMhr form, occurs with an observed rate constant of 0.22±0.04 s^{-1}, more than five orders of magnitude faster than that observed for autoxidation of the wild-type protein. The decomposition of the oxyL103NMhr is also faster, occurring with an observed rate constant of (2.4±0.1)X10^{-3} s^{-1}. Fig. 2 displays absorbance vs. log time plots for the second kinetic phases. We did not observe any UV–Vis spectral evidence for additional Mhr species (i.e. other than deoxy, oxy, or met forms), possibly indicative of oxidase activity for the L103V or L103N mutants. The met forms of the mutants do not react with hydrogen peroxide.

DeoxyMhr formation was studied [19] by dithionite scavenging of dissolved O_2 from solutions containing oxyMhr, O_2 (0.4–1.5 mM), and $Na_2S_2O_4$ (50–300 mM). The primary reductant in these reactions is the SO_2 radical, which rapidly equilibrates with S_2O_4 in aqueous

[4] The [N3] dependence of the rates of azide assisted autoxidation of oxyMhr and azide anation of metMhr reactions were measured simultaneously by mixing various concentrations of azide with a mixture of oxyMhr and metMhr. The observed rates of these reactions differ by more than two orders of magnitude at the lowest concentration of azide used and the kinetic steps can be easily resolved.

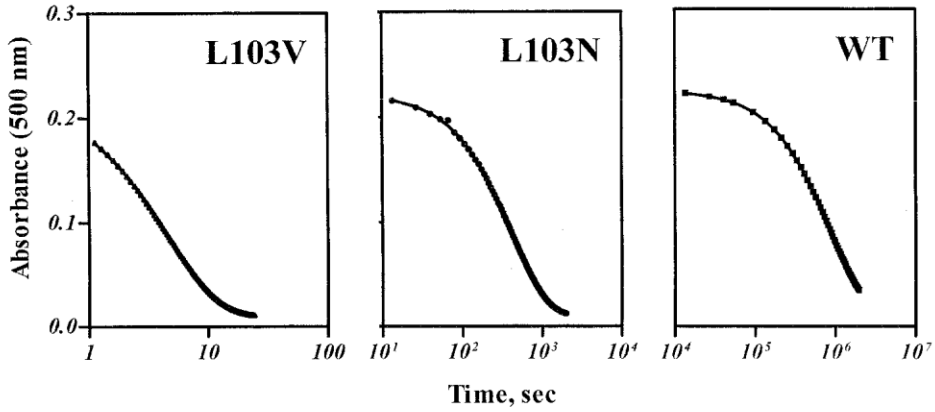

Fig. 2. Changes in absorbance (500 nm) vs. log time for the reaction (pH 8.0; 12°C; 1 bar) of O_2 with deoxymyohemerythrins. Autoxidation is observed following the formation of oxymyohemerythrins. WT, L103N, and L103V refer to the wild-type, Leu-103→Asn-103, and Leu-103→Val-103 proteins, respectively. Rate constants for autoxidation are shown in Table 1.

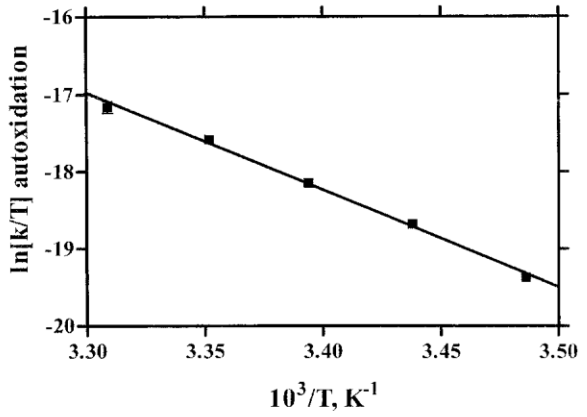

Fig. 3. Eyring plot of the observed rates (1 bar; pH 8.0) of solvolytic autoxidation ($k_{autoxid}$, ■) for wild-type oxymyohemerythrin.

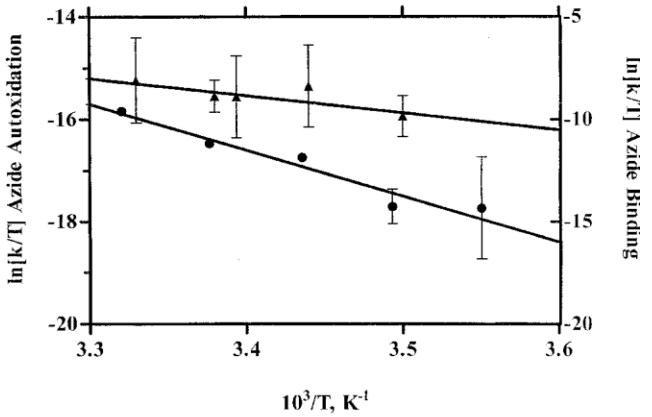

Fig. 5. Eyring plots of the temperature dependencies of the observed rates (1 bar; pH 8.0; 300 mM NaN_3) of azide binding to wild-type metmyohemerythrin (▲) and azide-assisted autoxidation of oxymyohemerythrin (●).

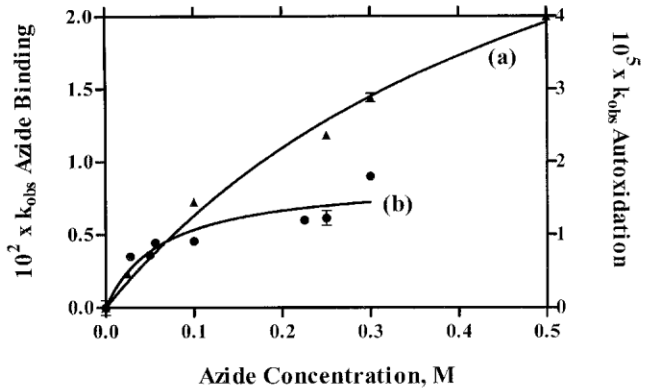

Fig. 4. Observed rate constants (s^{-1}, 21.5°C; 1 bar; pH 8.0) of (a) azide uptake by wild-type metmyohemerythrin (▲) and (b) azide-assisted autoxidation of oxymyohemerythrin (●). Both reactions exhibit saturation kinetics; hyperbolic rate expressions are shown in Table 2.

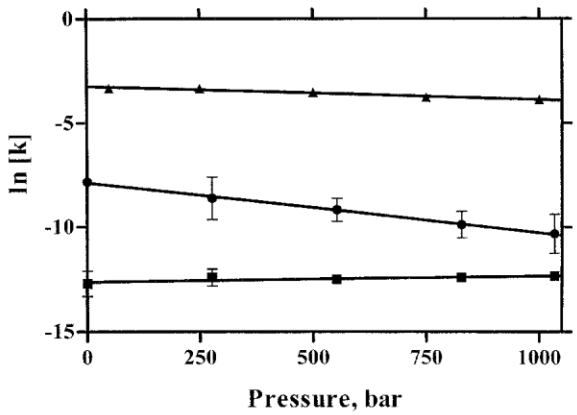

Fig. 6. Pressure dependencies (21.5°C; pH 8.0; 300 mM NaN_3) of the solvolytic autoxidation (■), azide-assisted autoxidation (●), and azide anation (▲) reactions of wild-type oxyMhr.

Table 1
Summary of rate data[a] for O_2 release and solvolytic autoxidation of oxymyohemerythrins

Parameter	O_2 release	Autoxidation
kWT(s^{-1}; 12°C; 1 bar)	55±4	$(9.1\pm0.1)\times10^{-7}$
kL103V (s^{-1}; 12°C; 1 bar)	Not determined	0.22±0.04
kL103N (s^{-1}; 12°C; 1 bar)	Not determined	$(2.4\pm0.1)\times10^{-3}$
$\Delta H^{\ddagger}$ (kcal mol^{-1})	+22±1	+24.1±0.7
$\Delta S^{\ddagger}$ (eu; 1 bar)	+28±4	+1±1
$\Delta V^{\ddagger}$ (cm^3 mol^{-1}; 21.5°C)	+28±3	−8±2

[a] Data are reported for pH 8.0. WT, L103V, and L103N denote the wild-type, Leu-103→Val-103, and Leu-103→Asn-103 oxymyohemerythrins, respectively. Activation parameters are for the wild-type protein. The autoxidation rate constant for the wild-type protein is calculated from the activation parameters at 12°C. Activation parameters for O_2 release are from Ref. [19].

solutions [34] (H_2O_2 is also scavenged). Sulfite, generated from the oxidation of dithionite, does not bind to the active site of Mhr; other products of the O_2 and $S_2O_4^2$ reaction do not interfere with the deoxygenation kinetics [35,36].[5] Temperature-dependent data (pH 8.0, 1 bar) are plotted in Fig. 3 for solvolytic autoxidation. The onset of thermal denaturation [37] occurs at —29°C, setting an upper limit to the temperature range employed in this study. Table 1 summarizes rate data[6], including volumes of activation, for these reactions.

Azide accelerates [38,39] the autoxidation process, as do other small anions (e.g. Cl-, F-, and CNO). The product of the azide-assisted autoxidation of oxyMhr is azidometMhr. This orange-colored adduct can also be produced by the direct anation of metMhr. In both cases, the observed rate exhibits a hyperbolic[7]; rather than a linear, dependence on [N3] (see Table 2). Both anation and azide-assisted autoxidation rate constants (kcaj were determined by fitting k_{obs} to an expression of the form $k_{calc}[N_3]/\{K_d+[N_3]j$. Fig. 4 displays the observed rates (21.5°C, 1 bar, pH 8.0) of azide anation and assisted autoxidation as a function of [N3]. The temperature dependencies (1 bar, pH 8.0, 300 mM NaN_3) of k_{obs} for azide-assisted autoxidation and k_{calc} for azide anation are shown in Fig. 5. The pressure dependencies (21.5°C, pH 8.0) of solvolytic autoxidation, azide-assisted autoxidation, and azide anation are displayed in Fig. 6. Table 2 summarizes the results of the azide experiments.

Table 2
Summary of rate data[a] for azidometMhr formation by anation of metMhr or azide-assisted oxyMhr autoxidation

Parameter	Anation	Autoxidation
k_{obs} (21.5°C; 1 bar)	$\frac{0.04\ [N_3^-]}{(0.5+[N_3^-])}$	$\frac{1.38\times10^{-5}\ [N_3^-]}{(0.038+[N_3^-])}$
$\Delta H^{\ddagger}$ (kcal mol^{-1})	+16±7	+17±2
$\Delta S^{\ddagger}$ (eu; 1 bar)	−10±7	−21±7
$\Delta V^{\ddagger}$ (cm^3 mol^{-1}; 21.5°C)	+15±2	+59±2

[a] Data are reported for pH 8.0. Activation parameters are reported for 300 mM NaN_3.

[5] O2 trapping, not reductive decay of the μ-1,2-peroxodiiron(III) active site, is shown to occur as the colorless deoxyMhr (diferrous μ-oxy) product is obtained (not the diferric metMhr).
[6] The relative rates for L1 03V and L1 03N autoxidation were inadvertently juxtaposed in Ref. [28].
[7] Azide anation of metMhr data have been reported before [28]; saturation kinetics for this reaction is only observed at relatively high azide concentrations.

4. DISCUSSION

The importance of protein conformational fluctuations has been noted describing the kinetic steps involved in the O_2 uptake and release reactions of Mhr and Hr [19,40]. That such fluctuations are of major importance in ligand binding and release is evident from an inspection of X-ray crystal structures [11–14] of various forms of these proteins: the absence of a static channel linking the protein active site with the solvent indicates that ligand substitutions must be multistep processes.

In the case of T. zostericola Mhr, the onset of thermal denaturation occurs at —29°C, setting the upper limit to the accessible temperature range for kinetic studies. This lowers somewhat the reliability of $\Delta S^{\ddagger}$ as a mechanistic indicator. More importantly, our results for Mhr (Tables 1 and 2, Ref. [19]) demonstrate that the sign of $\Delta S^{\ddagger}$ cannot be used to assert whether an observed rate represents ligand binding to Fe2 in the active site or elsewhere in the protein. For example, the step limiting the O_2 uptake rate likely involves [19] a protein fluctuation, rather than Fe–O bond formation. Additionally, measurements of metalloprotein activation volumes [41] can be done with more accuracy and also provide more useful probes of dynamics.

The activation parameters [19] for the release of O_2 by oxyMhr (Table 1) all reflect a rate-limiting step that involves a simple Fe–O bond dissociation. In particular, we note that $\Delta V^{\ddagger} = +28 \pm 3$ cm^3 mol^{-1}, which exactly corresponds to the value for the partial molar volume of O_2. Projahn et al. [42] also reported a positive $\Delta V^{\ddagger}$ for O_2 release by T. zostericola Hr, which they attributed to Fe2–O_2 bond breakage and/or reduction of Fe(III) to Fe(II).

The autoxidation of oxyMhr results in the formation of metMhr, and is believed to be accompanied by the release of hydrogen peroxide [1]. This process would be of little consequence in the case of wild-type oxyMhr, except for the fact that it is likely irreversible in vivo in the absence of reductase proteins. The contrasting signs of the activation volumes for O_2 release and autoxidation (pH 8.0) indicate that the rate-limiting steps of these reactions are markedly different — that for autoxidation is not dissociative (with respect to Fe2) in nature. The near-zero value for the autoxidation $\Delta S^{\ddagger}$ is consistent with the incoming nucleophile being some form of protein-associated water that has low mobility[8]. Interestingly, an internal water molecule has been found, associated with His-25 and other residues, in the X-ray structures of metMhrs [11,14]; water molecules are also observed hydrogen-bonded to the protein surface.

How does the protein minimize this autoxidation reaction? Refined X-ray crystal structures [11–13] of T. dyscrita azidomet- and oxyHrs, and T. zostericola azidometMhr place a leucine side chain in van der Waal's contact with the bound ligand. This amino acid residue (10^3 in Mhr) is conserved in all known Hr and Mhr sequences. O_2 uptake reactions of two deoxyMhr mutants, containing either valine or asparagine at position 103, were therefore studied by stopped-flow spectrophotometry. In both cases, the oxy adducts were found to be very unstable due to a surprisingly fast decay of the oxy adduct to yield met (diferric) products. In particular, shortening the side chain of residue 103 by one methylene linkage (L103V mutant) leads to a $\approx 2.3\ 3\ 10^5$ increase in the autoxidation rate. The valine side chain cannot be in Van der Waal's contact with bound oxygen as it is in the wild-type protein. The loss of steric shielding and/or greater accessibility of the solvent may be responsible for the increased rate.[9] We also previously noted [28] that the rate constant for azide anation increases for the L103V mutant relative to the wild-type Mhr, in keeping with this view. Computer graphics modelling [14,37] of Mhr shows that Fe2 can be accessed from the interhelical core (and thence from the solvent) once the side chain of Leu-103 is rotated appropriately. Hence, we regard this residue as a protein gate, whose function is to shield bound O_2 from nucleophilic displacement. A leucine gate has also been proposed to

[8] Solvolytic autoxidation resulting from attack on Fe2 by a water molecule from the bulk solvent would be expected to yield a DV‡ .0 and DS‡ ,0 (reminiscent of O2 uptake) [19]. This low mobility, protein-associated water may be located in the protein matrix or possibly bound to its surface.

[9] The spontaneous decomposition (autoxidation) of the mutant oxyMhrs is not believed to occur by reduction of the oxygen to water as none of the metMhrs show any reaction with H2O2, and H2O2 does not react with any of the oxyMhrs. There is also no kinetic evidence for additional intermediates that might be present after mixing.

be operative during methane monooxygenase turnover [43]. The 100-fold increase in rate constant for the autoxidation of the L103V Mhr mutant, relative to the rate constant for the L103N mutant, may reflect hydrogen bonding between bound hydroperoxide and the Asn-103 side chain (possibly involving a water bridge, as observed in the L103N hydroxometMhr structure) [14]. It has been suggested that the unusual stability of oxyMhr (and oxyHr) with respect to autoxidation is due to hydrogen bonding of the bound ligand with the oxo bridge [9]. Our results (Fig. 1 and Table 1) indicate this impression is incomplete, in agreement with recent kinetic work on model compounds [44]. Steric bulk imposed by the protein around the active site in oxyMhr and oxyHr (especially an aliphatic residue that is in van der Waal's contact with bound hydroperoxide) appears to be a considerable factor in determining the stability of the oxy adduct with respect to autoxidation; this feature of Mhr will be difficult to incorporate into oxyMhr model complexes.

In addition to water, small solutes can promote autoxidation of oxyMhr and oxyHr. Wilkins and coworkers [38,39] have noted that azide can also assist the autoxidation process, and proposed the following mechanism for azide-assisted autoxidation of oxyHr:

$$Hr([Fe(III,III)]O_2)_8 \leftrightarrow Hr([Fe(II,II)])_8 + 8O_2 \quad (3)$$

$$Hr([Fe(II,II)])_8 + 8HN_3 \leftrightarrow Hr([Fe(II,II)]N_3)_8 + 8H^+ \quad (4)$$

$$Hr([Fe(II,II)]N_3^-)_8 + 8O_2 \text{—>} Hr([Fe(III,III)]N_3)_8 + 8O_2^{2-} \quad (5)$$

The product of the last step (Eq. (5)), azidometHr, can also be produced by direct anation of metHr. The azide-assisted autoxidation and anation [28] reactions are also observed with Mhr. Azide-assisted autoxidation of oxyMhr and oxyHr is accelerated by acid (results not shown and Ref. [45]), indicating that the species entering the protein matrix is likely HN3. Since the first two steps are fast (see the Results section and Ref. [46]), this mechanism requires that the last step be rate determining. The initial step (Eq. (3)) of the Wilkins azide-assisted autoxidation mechanism was proposed [38] partly to explain a rapid bleaching of the hydroperoxo—>Fe^{III} charge-transfer transition that is responsible for the purple color of oxyMhr and oxyHr. This step cannot be operative unless O_2 is present in low concentration.[10] 10 More importantly, two-electron outer-sphere oxidation of azidodeoxyMhr by O_2 (Eq. (5)) is very unlikely to be concerted, as the Fe1 and Fe2 centers are nonequivalent. Two single-electron oxidation steps are also implausible, since the second would be thermodynamically unfavorable [47,48].

As Fig. 5 illustrates, saturation kinetics are observed for both azide anation of metMhr and azide-assisted catalysis of oxyMhr autoxidation. This suggests that azide binds/ interacts with the protein matrix prior to the step involving ligation to Fe2.[11] A minimal three-step mechanism is needed to discuss any ligand-binding reaction of a form of Mhr:

$$\mathbf{Mhr + L \rightleftarrows L,Mhr} \quad (6)$$

$$\mathbf{L,Mhr \rightleftarrows L,*Mhr} \quad (7)$$

$$\mathbf{L,*Mhr \rightleftarrows L\,*Mhr} \quad (8)$$

[10] We did not observe rapid bleaching of oxyMhr upon azide addition. The equilibrium constant for the $HrO_2 + N_3 \leftrightarrow HrN_3 + O_2$ reaction at 25°C and pH 6.3 was determined to be 0.017 [38]. Low O_2 and relatively high N_3 concentrations would, therefore, be required for rapid bleaching to be observed.

[11] Although both low and high affinity anion binding sites were described for Hr in Ref. [49], the Kd for azide-anation of metMhr is so large that it could represent non-specific binding. The interpretation of saturation kinetics for azide anation as anion binding in a rapid pre-equilibrium step, prior to a protein gating step, is supported by the fact that the activation volumes for azide anation and azide-assisted autoxidation are different from each other and from the activation volume for O_2 uptake [19].

Here, L is a generic incoming ligand, and *Mhr denotes an alternate conformation of Mhr. Hence, Eq. (7) represents a protein-gating step that permits ligand entry into the ligand-binding pocket. Eq. (8) denotes the final step, involving a ligand substitution at Fe2. Azide entries into both metMhr and oxyMhr are characterized by relatively large, positive values for $\Delta V^{\ddagger}$ (the activation volume for solvolytic autoxidation is negative). This indicates that the rate-limiting step of neither mechanism is associative (this would require negative activation volumes) with respect to ligand substitution at the Fe2 center. Since an expanded Fe2 coordination sphere is not indicated, these activation volumes most likely reflect protein dynamics.

In oxyMhr, hydroperoxide resides in the cavity between the Fe–O–Fe core and Leu-103. The O_2 binding pocket of oxyMhr is presumably more tightly packed than is that of metMhr, as indicated by the X-ray crystal structures [12,13] of analogous T. dyscrita met- and oxyHrs, accounting for the much larger activation volume for the azide-assisted autoxidation reaction. Our view of the solvolytic and azide-assisted autoxidations of oxyMhr is schematically depicted in Fig. 7. There may be more than one protein

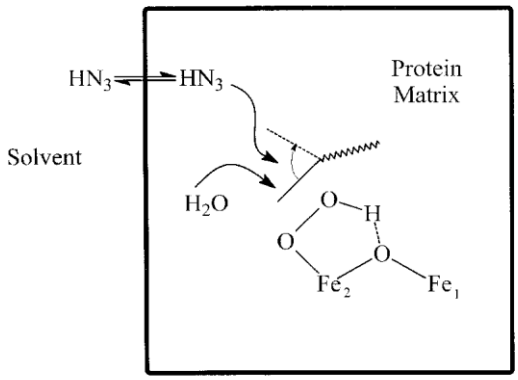

Fig. 7. Proposed pathways for autoxidation. In the rate-limiting step for solvolysis, protein-associated water (which may be in the protein interior or bound to the surface) or azide influences the extent of protein conformational gating prior to inner-sphere complex formation with Fe2.

'gate' for the reactions discussed in this study, but at least one residue, leucine-103, has been shown to strongly influence the stability of oxyMhr in this work, as well as influence azide uptake kinetics [28].

The traditional view of metalloproteins, as 'metal ions in disguise', has strongly influenced mechanistic studies of ligand binding. However, X-ray structures of Hrs and Mhrs show that their active sites are not directly accessible to the solvent, indicating that protein side-chain motions play key roles in ligand binding by these proteins. In these situations, the mechanistic significance, with respect to the metal-ion active sites, of variations in temperature and incoming solute becomes blurred. For example, $\Delta H^{\ddagger}$ for azide uptake and azide-assisted autoxidation are identical within experimental error (as are $\Delta S^{\ddagger}$ values for these reactions). The activation volumes clearly show that the rate-limiting steps for these reactions do not involve Fe2– N_3 bond formation.

Similar considerations apply to other metalloproteins. In the case of myoglobin, ongoing experiments [50,51], using site-directed mutagenesis and photoinduced ligand (principally O_2 and CO) recombination kinetics, are elucidating channels for ligand entry and egress. The 1.5-A X-ray crystal structure [52] of photolyzed carbonmonoxymyoglobin dramatically illustrates the importance of protein dynamics in determining ligand-substitution mechanisms. Recent X-ray crystal structures of other metalloproteins, including Lumulus polyphemus hemocyanin [53], copper amine oxidases [54,55], cytochrome c oxidases [56–58], Klebsiella aerogenes urease [59], and methane monooxygenase [60], indicate that the problem of ligand access to buried active sites is more common than previously realized.

4.1. Abbreviations

azidodeoxyMhr azidodeoxymyohemerythrin

azidometHr	azidomethemerythrin
azidometMhr	azidometmyohemerythrin
deoxyHr	deoxyhemerythrin
deoxyMhr	deoxymyohemerythrin
Hr	hemerythrin
Mhr	myohemerythrin
oxyHr	oxyhemerythrin
oxyMhr	oxymyohemerythrin
T. dyscrita	Themiste dyscrita
T. zostericola	Themiste zostericola

ACKNOWLEDGEMENTS

We thank Professor Rudi van Eldik (Universität Erlangen-Niirnberg, Germany) for helpful discussions. This research was supported by the Department of Energy, Office of Basic Energy Sciences (EME) and National Institutes of Health Grant GM 43507 (WRE).

REFERENCES

[1] G.B. Jameson, J.I. Ibers, in: I. Bertini, H.B. Gray, S.J. Lippard, J. Valentine (Eds.), Bioinorganic Chemistry, University Science Press, Mill Valley, CA, 1994, pp. 167–252.
[2] P.C. Wilkins, R.G. Wilkins, Coord. Chem. Rev. 79 (1987) 195–214.
[3] R.G. Stenkamp, Chem. Rev. 94 (1994) 715–726.
[4] J. Sanders-Loehr, in: T.M. Loehr (Ed.), Iron Carriers and Iron Proteins, VCH, New York, 1989, pp. 373–466.
[5] D.M. Kurtz Jr., Chem. Rev. 90 (1990) 585–606.
[6] J.B. Vincent, G.L. Olivier-Lilley, B.A. Averill, Chem. Rev. 90 (1990) 1447–1467.
[7] L. Que Jr., A.E. True, Prog. Inorg. Chem. 38 (1990) 97–200.
[8] R.G. Wilkins, Chem. Soc. Revs. 1 (1990) 171–178.
[9] A.L. Feig, S.J. Lippard, Chem. Rev. 94 (1994) 759–805.
[10] Y. Lindqvist, W. Huang, G. Schneider, J. Shanklin, EMBO J. 15 (1996) 4081–4092.
[11] M.A. Holmes,I. Le Trong, S. Turley, L.C. Sieker, R.E. Stenkamp, J. Mol. Biol. 218 (1991) 583–593.
[12] S. Sheriff, W.A. Hendrickson, J.L. Smith, J. Mol. Biol. 197 (1987) 273–296.
[13] M.A. Holmes, R.E. Stenkamp, J. Mol. Biol. 220 (1991) 723–737.
[14] L.J. Martins, C.P. Hill, W.R. Ellis Jr., Biochemistry 36 (1997) 7044–7049.
[15] A.K. Shiemke, T.M. Loehr, J. Sanders-Loehr, J. Am. Chem. Soc. 106 (1984) 4951–4956.
[16] A.K. Shiemke, T.M. Loehr, J. Sanders-Loehr, J. Am. Chem. Soc. 108 (1986) 2437–2443.
[17] R.C. Reem, J.M. McCormick, D.E. Richardson, F.J. Devlin, P.J. Stephens, R.L. Musselman, E.I. Solomon, J. Am. Chem. Soc. 111 (1989) 4688–4704.
[18] R.E. Stenkamp, L.C. Sieker, L.H. Jensen, J.D. McCallum, J. Sanders-Loehr, Proc. Natl. Acad. Sci. USA 82 (1985) 713–716.
[19] C.R. Lloyd, E.M. Eyring, W.R. Ellis Jr., J. Am. Chem. Soc. 117 (1995) 11993–11994.
[20] R.E. Utecht, D.M. Kurtz Jr., Inorg. Chem. 24 (1985) 4559–4561.
[21] F. Bonomi, R.C. Long, D.M. Kurtz Jr., Biochim. Biophys. Acta 999 (1989) 147–156.
[22] W.H. Armstrong, S.J. Lippard, J. Am. Chem. Soc. 105 (1983) 4837–4838.
[23] K. Wieghardt, K. Pohl, W. Gebert, Angew. Chem., Intl. Ed. Engl. 22 (1983) 727–728.
[24] T. Ookubo, H. Sugimoto, T. Nagayama, H. Masuda, T. Sato, K. Tanaka, Y. Maeda, H. Okawa, Y. Hayashi, A. Uehara, M. Suzuki, J. Am. Chem. Soc. 118 (1996) 701–702.
[25] Y. Dong, S. Yan, V.G. Young Jr., L. Que Jr., Angew. Chem., Intl. Ed. Engl. 35 (1996) 618–620.
[26] B. Eulering, M. Schmidt, U. Pinkernell, U. Karst, B. Krebs, Angew. Chem., Intl. Ed. Engl. 35 (1996) 1973–1974.
[27] T.J. Mizoguchi, S.J. Lippard, J. Am. Chem. Soc. 120 (1998) 11022–11023.

[28] G.M. Raner, L.J. Martins, W.R. Ellis Jr., Biochemistry 36 (1997) 7037–7043.
[29] R.C. Neuman Jr., W. Kauzmann, A. Zipp, J. Phys. Chem. 77 (1973) 2687–2691.
[30] R.M.C. Dawson, D.C. Elliot, W.H. Elliot, K.M. Jones, Data for Biochemical Research, Clarendon Press, Oxford, 1986.
[31] W.J. LeNoble, R. Schlott, Rev. Sci. Instrum. 47 (1976) 770–771.
[32] Q. Ji, E.M. Eyring, R. van Eldik, K.B. Reddy, S.R. Goates, M.L. Lee, Rev. Sci. Instrum. 66 (1995) 222–226.
[33] R. van Eldik, W. Gaede, W. Wieland, J. Kraft, M. Spitzer, D.A. Palmer, Rev. Sci. Instrum. 64 (1993) 1355–1357.
[34] C. Creutz, N. Sutin, Inorg. Chem. 13 (1974) 2041–2043.
[35] P.C. Harrington, D.J.A. deWaal, R.G. Wilkins, Arch. Biochem. Biophys. 191 (1978) 444–451.
[36] D.J.A. deWaal, R.G. Wilkins, J. Biol. Chem. 251 (1976) 2339–2343.
[37] L.J. Martins, PhD dissertation, University of Utah, 1994.
[38] Z. Bradic,~ R. Conrad, R.G. Wilkins, J. Biol. Chem. 252 (1977) 6069–6075.
[39] Z. Bradic,~ P.C. Harrington, R.G. Wilkins, in: W.S. Caughey (Ed.), Biochemical and Clinical Aspects of Oxygen, Academic Press, New York, 1979, pp. 557–571.
[40] D. Lavalette, C. Tetreau, J.-C. Brochon, A. Livesey, Eur. J. Biochem. 196 (1991) 591–598.
[41] K. Hermans, in: R. van Eldik (Ed.), Inorganic High Pressure Chemistry: Kinetics and Mechanism, Elsevier, Amsterdam, 1986, pp. 339–393.
[42] H.-D. Projahn, S. Schindler, R. van Eldik, D.G. Fortier, C.R. Andrew, A.G. Sykes, Inorg. Chem. 34 (1995) 5935–5941.
[43] A.C. Rosenzweig, H. Brandstetter, D.A. Whittington, P. Nordlund, S.J. Lippard, C.A. Frederick, Proteins Struct. Funct. Genet. 29 (1997) 141–152.
[44] A.L. Feig, M. Becker, S. Schindler, R. van Eldik, S.L. Lippard, Inorg. Chem. 35 (1996) 2590–2601.
[45] D.R. Meloon, R.G. Wilkins, Biochemistry 15 (1976) 1284–1290.
[46] P.C. Wilkins, R.G. Wilkins, Biochim. Biophys. Acta 912 (1987) 48–55.
[47] F.A. Armstrong, P.C. Harrington, R.G. Wilkins, J. Inorg. Biochem. 18 (1983) 83–91.
[48] J.A. Fee, J.S. Valentine, in: A.M. Michelson, J.M. McCord, I. Fridovich (Eds.), Superoxide and Superoxide Dismutases, Academic Press, London, 1977, pp. 19–60.
[49] K. Garbett, D.W. Darnell, I.M. Klotz, Arch. Biochem. Biophys. 142 (1971) 471–480.
[50] M.F. Perutz, Trends Biochem. Sci. 14 (1989) 42–44.
[51] J.S. Olson, G.N. Phillips Jr., J. Biol. Chem. 271 (1996) 17593– 17596.
[52] H. Hartmann, S. Zinser, P. Komninos, R.T. Schneider, G.U. Nienhaus, F. Parak, Proc. Natl. Acad. Sci. USA 93 (1996) 7013– 7016.
[53] B. Hazes, K.A. Magnus, C. Bonaventura, J. Bonaventura, Z. Dauter, K.H. Kalk, W.G.J. Hol, Protein Sci. 2 (1993) 597–619.
[54] M.R. Parsons, M.A. Convery, C.M. Wilmot, K.D.S. Yadav, V. Blakeley, A.S. Corner, S.E. V Phillips, M.J. McPherson, P.F. Knowles, Structure 3 (1995) 1171–1184.
[55] V. Kumar, D.M. Dooley, H.C. Freeman, J.M. Guss, I. Harvey, M.A. McGuirl, M.C.J. Wilce, V.M. Zubak, Structure 4 (1996) 943–955.
[56] S. Iwata, C. Ostermeier, B. Ludwig, H. Michel, Nature 376 (1995) 660–669.
[57] T. Tsukihara, H. Aoyama, E. Yamashita, T. Tomizaki, H. Yamaguchi, K. Shinzawa-Itoh, R. Nakashima, R. Yaono, S. Yoshikawa, Science 269 (1995) 1069–1074.
[58] T. Tsukihara, H. Aoyama, E. Yamashita, T. Tomizaki, H. Yamaguchi, K. Shinzawa-Itoh, R. Nakashima, R. Yaono, S. Yoshikawa, Science 272 (1996) 1136–1144.
[59] E. Jabri, M.B. Carr, R.P. Hausinger, P.A. Karplus, Science 268 (1995) 998–1004.
[60] A.C. Rosenzweig, C.A. Frederick, S.J. Lippard, P. Nordlund, Nature 366 (1993) 537–543.